Towards Improved Sensor Systems for Bridge Structural Health Monitoring

Alan J. Ferguson[1], Roger Woods[1], David Hester[2]
[1]School of Electronics, Electrical Engineering and Computer Science, Queen's University Belfast, Northern Ireland
[2]School of Natural and Built Environment, Queen's University Belfast, Northern Ireland
email: {aferguson29, r.woods, d.hester}@qub.ac.co.uk

ABSTRACT: Taking long-term measurements on in-service bridges is challenging due to the lack of easy access to power and communications. Whilst all-in-one, portable sensor data loggers act to address these challenges, they still lack the flexibility to meet evolving measurement needs. This paper presents the design and implementation of a highly flexible, modular sensor system for bridge structural health monitoring research, which has an emphasis on customisability and extensibility to allow it to meet evolving challenges. The architecture incorporates interchangeable sensor modules that allows data acquisition to an on-board Secure Digital card, with timing and synchronisation provided by global positioning system and a real-time clock chip and remote system monitoring and control utilising LoRaWAN. A prototype system has been developed and tested in both laboratory and field trials.

KEY WORDS: Sensor Systems; Data Acquisition; Time-Synchronisation; Embedded System Architecture.

1 INTRODUCTION

Field measurements are a key component of various structural health monitoring approaches [1]; however, collecting long-term data on bridge structures is challenging. Typically, traditional measurement setups require sensors, a data acquisition system or logger, and a computer. For long-term installation on bridges, this presents a number of problems: (i) power and/or communications are rarely available, (ii) the equipment is not typically designed for outdoor conditions, and (iii) it is quite expensive.

Hence, the recent availability of some relatively low-cost, portable, all-in-one sensor data logging systems on the market has been welcome. In effect, the manufacturers have integrated the sensors, data-acquisition hardware, a microcontroller, and storage (memory card) onto a single printed circuit board (PCB) which is packaged within a robust, waterproof casing.

Whilst the resultant, commercial products are relatively easy to use, this comes at the cost of one or more limitations in: (a) the performance of both the sensors themselves, e.g. resolution, or overall system, e.g. battery life; (b) adaptability, i.e. it cannot readily change sensors due to deterioration, damage or changing requirements, or alter logging software; and (c) features such as time synchronisation may be absent, or fail to interoperate with other manufacturer's hardware.

This study looks at the design, implementation, and evaluation of an innovative sensor system that emphasises customisability and extensibility to ensure the system has the adaptability to meet the challenges of changing research needs in the future. Section 2 covers specific aspects of the system design. Section 3 provides details of laboratory and field testing conducting on the system, with Section 4 presenting the results from these. Finally, conclusions are given in Section 5.

2 SENSOR SYSTEM

The key focus of this work has been to develop a system design with future iterative extension and customisation in mind. Therefore, by adopting an embedded system engineering approach, a modular architecture (Figure 1) was developed to cover the main sensor system functionality. Features include: (i) sensing, (ii) time synchronised data acquisition and storage, and (iii) remote device status monitoring and control; with each of the aspects covered in Sections 2.1 to 2.4.

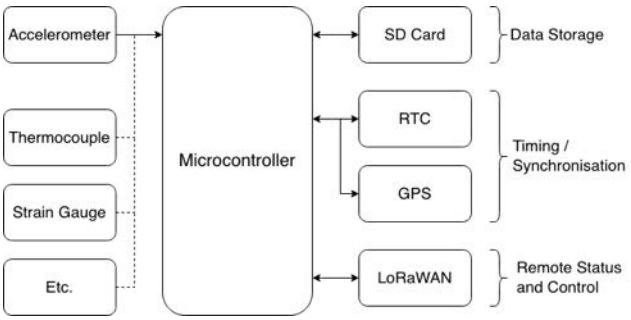

Figure 1: High-level system architecture overview.

2.1 Interchangeable Sensor Modules

Integrating a variety of sensors to meet changing system requirements can present a significant barrier, particularly if each new integration necessitates the redesign and verification of large parts of the system hardware, i.e. circuits and PCB layouts. Hence, the sensor front-end has been modularised, and placed on a separate expansion card. This means that only the sensor card needs to be redesigned for each new sensor integration with the system, and also allows the main board to be reused with each iteration.

When considering the design of the expansion cards, the choice of an appropriate interfacing mechanism to both mechanically and electrically interconnect the main board and expansion card is important. For this, a range of board-to-board connectors were considered such as card-edge connectors; however, in the end many of these were found unsuitable for the interface due to their relatively high cost, and poor

mechanical stability that these provided. A custom solution was therefore developed based on cheap, and ubiquitous, "pin header" connectors. By arranging these as shown in Figure 2, a sensor expansion card can be secured stably in a mezzanine arrangement (i.e. parallel and vertically offset from the main board) via soldering.

To determine what electrical connections to provide onto the expansion card, a range of commercially available sensor modules were evaluated, and the connections described in Table 1 represent the common set needed to allow operation of these.

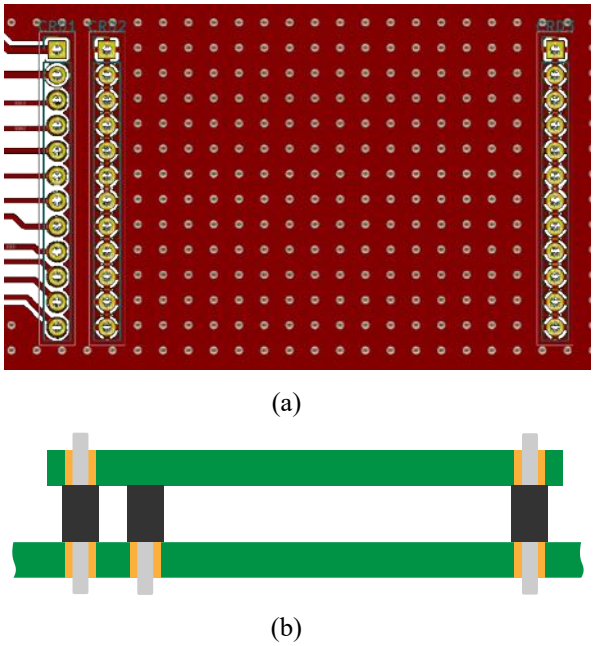

(a)

(b)

Figure 2: Detail of (a) PCB layout for sensor card interface, and (b) cross sectional diagram showing the mezzanine configuration of the sensor card when installed.

Table 1: Outline of the various electrical interfaces provided to the sensor expansion card.

Electrical Interface Connection to Card	**Purpose**
Power (3v3) + Ground	Supply power to components on expansion card
Analog Ground	Enable use of microcontroller (µC) on-board analog-digital converters for measurements.
Inter-Integrated Circuit (I2C)	Communication with common digitally interfaced components.
Serial Peripheral Interface (SPI)	Communication with common digitally interfaced components.
General Purpose Input-Output (GPIO)	Analog input and programmatic digital input and output from µC

2.2 Data Acquisition and Logging

The process of data acquisition is largely separated into two aspects, (1) sensing, i.e. getting a measurement value from the sensor at a desired sampling frequency along with an accurate time stamp for this; and (2) logging the samples (of sensor values and timestamps) to the storage medium, in this case, a micro-Secure Digital (SD) card.

However, writing to log files on the SD card is a blocking operation, and can halt all other functionality of the microprocessor. Therefore, this can lead to missed samples and jitter in the sampling frequency. To get around this, the operations of sensing and logging are implemented using two separate threads resulting in a producer-consumer model. Data is "produced" by the sensing thread retrieving data from the relevant sensor via SPI or I2C, and placed in a shared first-in-first-out (FIFO) buffer; the data in the FIFO is then "consumed" by the logging thread writing the data to the SD card. Due to these operations being performed within separate threads, this allows the sensing operations (as well as other system functionality) to carry on regardless of the blocking status of the logging thread and any related SD card write calls.

A summary of the process carried out by these 2 threads is shown below in the UML sequence diagram in Figure 3 (Note that operations within loop frame occur repeatedly).

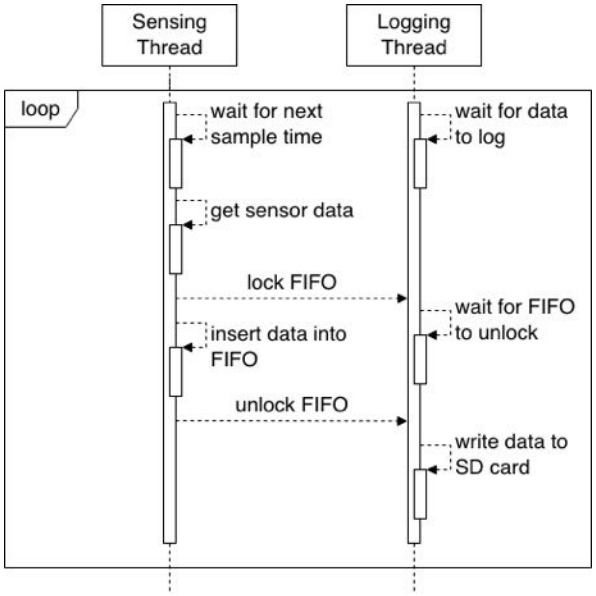

Figure 3: Sequence diagram showing overview of sensing thread and logging thread interactions.

The data passed to the "consumer" thread via the FIFO consists of that sampling instants sensor data, and a timestamp (obtained from the current timestamp maintained by the timing thread discussed in the next section). This data is then formatted as Comma Separated Values (CSV) at the point of being logged to the SD card. The sensor data is stored as the raw binary values retrieved from the sensors to minimise the processing time required to handle each sample; therefore, enabling faster sampling operation and reducing processor power consumption as this can increase processor idling time.

2.3 Data Acquisition Timestamping and Synchronisation

For this aspect of the system design, two different technologies have been utilised to tackle the 2 main parts of this challenge. Firstly, a Real-Time Clock (RTC) chip is incorporated to provide a low power, yet highly stable and accurate timing source local to each sensor node. Secondly, Global Positioning

System (GPS) is used as a global clock source for all sensor nodes to synchronise their internal clocks/timestamps against.

The choice of the RTC and GPS combination is partly due to the ease of configuration this allows. It means that each sensor node can be configured independently with no network or device configuration required to deploy and synchronise multiple sensor nodes, due to the almost "plug and play" nature of GPS time synchronisation (provided good sky coverage can be obtained).

2.4 Remote Monitoring and Control

One of the challenges of long-term field monitoring is needing to periodically visit the monitoring location to check the continued system operation. Whilst this may be acceptable for small deployments, it becomes less manageable at larger scales, potentially covering multiple localities.

Therefore, a core aspect of the sensor platform functionality was to enable remote monitoring and control (Figure 4). This is achieved using the capabilities provided by the Things Connected network [2], which is partnered with the global The Things Network (TTN) [3]. The wireless communication is carried out over LoRaWAN [4], a media access control protocol for wide area networks such as sensor deployments. It is designed to allow low-powered devices to communicate with Internet-connected applications over long-range wireless connections

Each sensor node at user-defined intervals will send status messages and these are routed to an endpoint on TTN. At the TTN endpoint messages are converted into raw data, which can be accessed directly via a web portal, or integrated into other systems via the TTN application programming interface (API). Each of these status messages contain, (i) battery voltage, (ii) data storage capacity remaining, (iii) any error codes encountered in the last recording period.

Additionally, downlink messages (sent to the sensor nodes) are utilised to provide remote management and control functionality. For example, this allows the sensor system to be scheduled remotely to turn on and off at specific times to optimise recording windows (e.g. possibly turning off at night when less ambient vibration occurs). Thus, enhancing the devices' power consumption as the system could be optimised to enter a low power state during the non-recording windows; therefore, enabling longer operation between battery replacements.

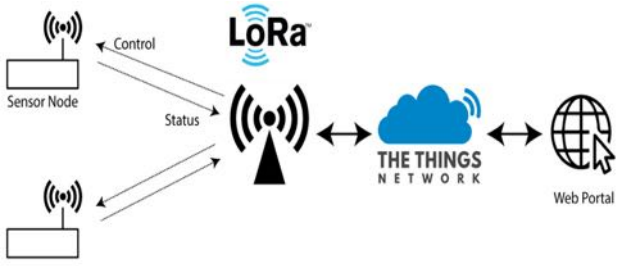

Figure 4: Overview of the data flow to and from sensor nodes and end users interacting through a web portal, via The Things Network and LoRa network.

3 EXPERIMENT SETUP

To test the system's performance a variety of experiments were carried out both in laboratory conditions and in-field. An initial prototype based on the system design presented in Section 2 was developed (Figure 5). For comparison this prototype was tested alongside a commercially available acceleration data logger, a Multifunction Extended Life (MEL) Data Logger [5]. These tests have focused on the sensing aspect, as the MEL logger does not offer the additional functionalities such as time synchronisation.

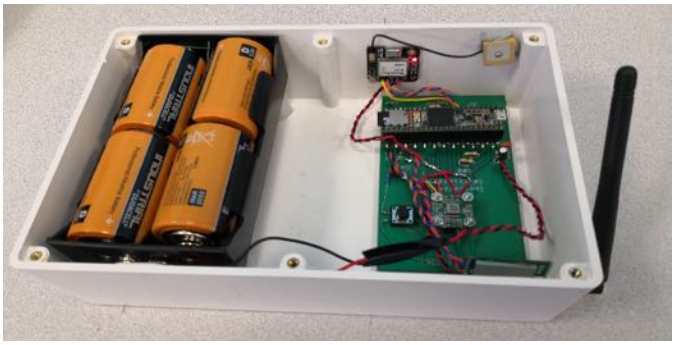

Figure 5: Initial system prototype with lid of enclosure removed showing main board, sensor module (ADXL355), GPS and LoRa transceiver; power supply circuit board and RTC are located under battery holder.

3.1 Laboratory Testing

Two different tests were performed with both systems spatially co-located, Firstly, static tests were carried out with the systems sitting on a solid concrete slab floor, with care taken to minimise any sources of external vibration. The resultant measurements are then analysed both for acceleration noise spectra and low-frequency noise (velocity random walk) which is determined by integration. Low-frequency noise was evaluated as this is a key aspect of operation [6], and can be mitigated by good sensor system design.

Secondly, dynamic tests were carried out with the systems mounted at the quarter-span point of a simply supported wooden beam as shown in Figure 6.

Figure 6: Simply-supported beam used for dynamic tests with data logger at the quarter-span point.

(a)

(b)

Figure 7: View of (a) A6 Toome Bridge from eastern aspect (photo: Kenneth Allen CC BY-SA 2.0), and (b) placement of the prototype system (left) and existing MEL logger (right) on the parapet of the bridge with enclosure lids removed.

3.2 Field Trial

As well as the laboratory testing described in the previous subsection, a field trial of a prototype system was carried out on the A6 Toome bridge between Belfast and Derry (pictured in Figure 7 (a)). Unfortunately, due to a component failure on one of the prototypes at the time of the field trial, these results are obtained using a prototype fitted with an InvenSense MPU-6050 accelerometer [7]; this having a lower resolution and higher noise than the ADXL355 used for the laboratory testing.

4 RESULTS AND DISCUSSION

The resultant acceleration graphs for both the system prototype and MEL for the static noise test (Section 4.1), dynamic testcase (Section 4.2) and finally results from the field trial on the A6 Toome bridge (Section 0) are presented and discussed.

4.1 Static Noise Test

The acceleration time histories obtained during the static test for both the prototype and MEL logger are shown in Figure 8 (a); with the corresponding noise spectra obtained using Welch's method presented in Figure 8 (b). From the noise spectra, the MEL shows a relative flat profile at lower frequencies followed by a roll-off indicative of some internal filtering; while the prototype exhibits a more typical 1/f noise profile, with low frequency noise dominating.

One of the challenges when designing sensor systems is the difference often observed between sensor metrics quoted in datasheets and the actual sensor performance when integrated into a final product. This difference is due to the values found in datasheets being measured in idealised conditions in laboratories. However, once these devices are placed in non-ideal circuits, alongside other components which inherently produce their own intrinsic noise and effects, the performance gap emerges.

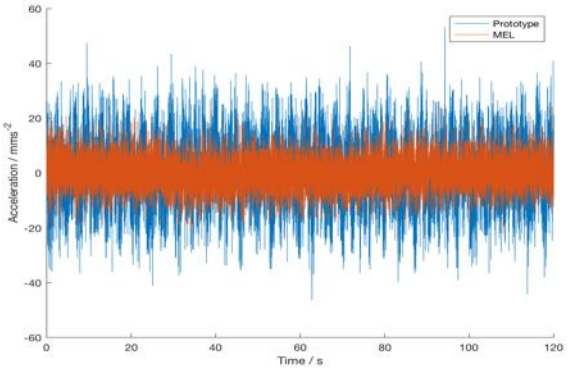

(a)

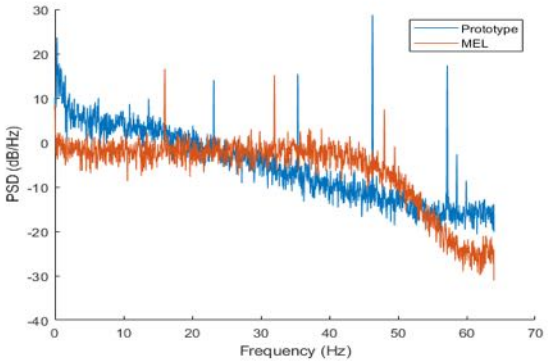

(b)

Figure 8: Results of static lab test showing (a) vertical acceleration recorded using MEL logger and system prototype; (b) power spectral density estimate of signals obtained using Welch's method.

Figure 9 shows the velocity random walk obtained for the recorded acceleration signals during the static test, wherein both systems performed similarly. Table 2 presents a summary of the datasheet noise spectral densities of the accelerometer used in the MEL (Kionix KXRB5-2050), and the ADXL355 used in our system prototype, versus the measured values from this testing. From these results, it can be seen that the measured values are worse than the quoted sensor noise performance, and that our system prototype performed comparatively worse. However, unlike the MEL, which as a commercial product offers effectively no scope to improve the noise performance, our system offers the opportunity to improve of this aspect in future system design iterations. Potential avenues to address this short-coming are decreasing overall system power supply noise, and increasing grounding and isolation of the sensor expansion card.

Table 2: Summary of accelerometer noise spectral densities from datasheet versus measured values.

Accelerometer	**Datasheet Noise Spectral Density** $(\mu g/\sqrt{Hz})$	**Measured Noise Spectral Density** $(\mu g/\sqrt{Hz})$
MEL [8]	45	621
ADXL355 [9]	20	1300

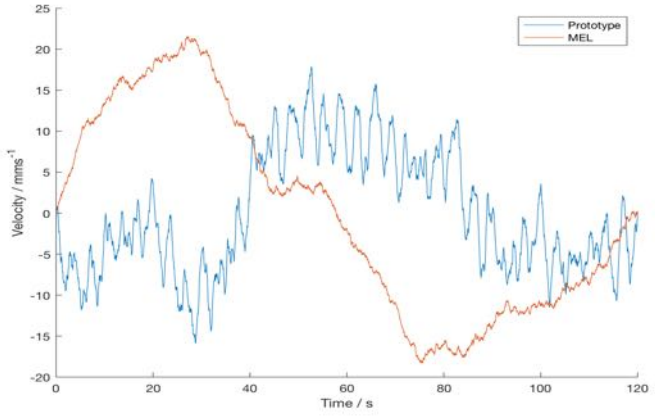

Figure 9: Random velocity walk of acceleration signals recorded during static lab test for MEL and prototype.

4.2 *Dynamic Test*

Acceleration time histories recorded during the dynamic test for both the prototype (ADXL355) and MEL logger are shown in Figure 10 (a) and (b), with detail shown of a free decay for the corresponding sensors in Figure 10 (c) and (d).

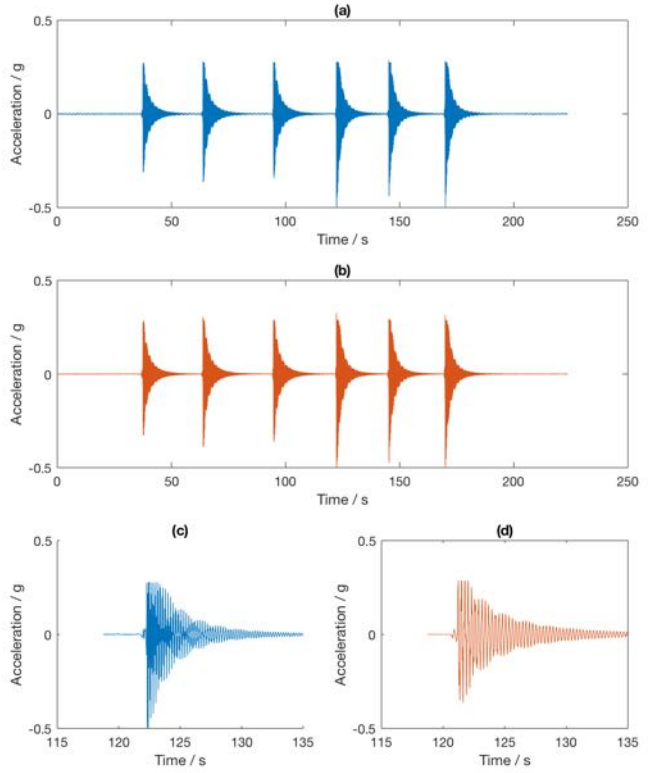

Figure 10: Graphs of acceleration data captured during dynamic lab test by (a) the system prototype, and (b) the MEL; and an enlarged view of the 4th free decay for the prototype system (c), and the MEL logger (d).

Based on the recorded acceleration profiles, natural frequencies where extracted using a Welch's power spectral density estimate and the results of this can be seen in Table 3.

Table 3: Summary of 1st Mode Frequencies extracted from dynamic test for MEL and Prototype System.

System	**1st Mode Frequency (Hz)**
MEL	2.08
Prototype with ADXL355	2.11

4.3 *Field Trial*

The acceleration time histories recorded during the field trial using the prototype system (MPU-6050) and MEL logger are shown in Figure 11 (a); with a zoomed in view presented in Figure 11 (b), and in broad terms the prototype system captures the acceleration reasonably, albeit with noticeably more noise.These acceleration signals were then examined in the frequency domain (Figure 12).

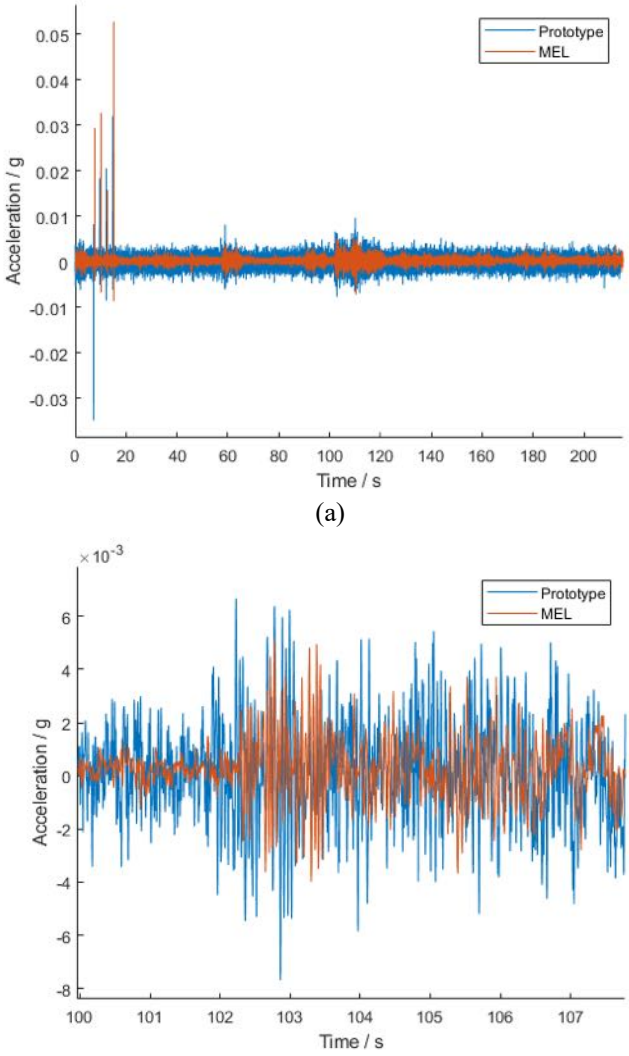

Figure 11: Graphs of (a) acceleration data captured during the field trial; (b) enlarged view of acceleration time history.

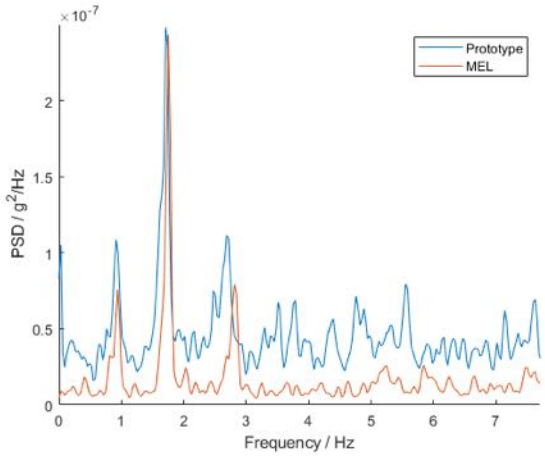

(a)

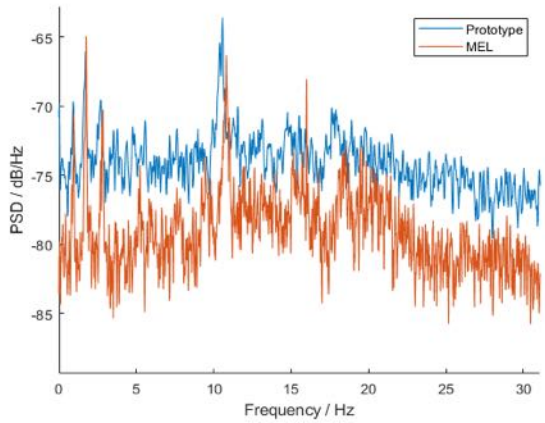

(b)

Figure 12: Power spectral density estimates via Welch's method of the acceleration signs from the field trial, recorded using both MEL and prototype systems.

From Figure 12 (a), the first 3 modes can be clearly seen in both signals at around 0.93Hz, 1.73Hz, and 2.70Hz. However, whilst the frequencies can be extracted, both systems give slightly different values, primarily caused by the lack of clock synchronisation between the 2 systems, In Figure 12 (b), the relatively high noise levels of both signals can be seen over a broader frequency range, which can make detection of lower amplitude modes harder.

5 CONCLUSION

This paper covers the development of a sensor system design, tailored to meet the challenges of field measurements from structures such as bridges. To ensure the system has the customisability and enable future extension, a modular architecture has been developed and the major components of this are described. An initial prototype based on this system architecture has been tested through both laboratory and field trials. Whilst the results from this initial prototype does not meet the performance of the commercial system, mode frequencies were successfully extracted, and it should be noted that the goal of this work was showing the feasibility of the flexible, sensing system architecture. Based on the learning from the initial prototype, future work will seek to improve the performance of the system through an iterative design process; for example, focusing on improving sensor card performance by increasing isolation and grounding on the expansion card or decreasing system power supply noise.

ACKNOWLEDGMENTS

The authors would like to acknowledge the technical staff from School of Electronics, Electrical Engineering and Computer Science, QUB for their assistance with the manufacturing of the system prototypes. Also, we would like to thank Connor O'Higgins from School of Natural and Built Environment, QUB for his assistance with the field trial.

REFERENCES

[1] S. Ye, X. Lai, I. Bartoli, and A. E. Aktan, 'Technology for condition and performance evaluation of highway bridges', *J Civil Struct Health Monit*, May 2020, doi: 10.1007/s13349-020-00403-6.

[2] 'Digital Catapult - Digital Catapult LPWAN Testbed'. https://www.digicatapult.org.uk/for-startups/other-programmes/things-connected (accessed May 29, 2020).

[3] 'The Things Network'. https://thethingsnetwork.org/ (accessed May 29, 2020).

[4] LoRa Alliance, 'LoRaWAN™1.1 Specification'. Oct. 11, 2017, Accessed: May 26, 2020. [Online]. Available: https://lora-alliance.org/sites/default/files/2018-04/lorawantm_specification_-v1.1.pdf.

[5] 'Multifunction Extended Life Data Logger'. http://www.gcdataconcepts.com/mel.html (accessed May 29, 2020).

[6] D. Hester, J. Brownjohn, M. Bocian, and Y. Xu, 'Low cost bridge load test: Calculating bridge displacement from acceleration for load assessment calculations', *Engineering Structures*, vol. 143, pp. 358–374, Jul. 2017, doi: 10.1016/j.engstruct.2017.04.021.

[7] InvenSense Inc., 'MPU-6000 and MPU-6050 Product Specification'. Aug. 19, 2013, [Online]. Available: https://invensense.tdk.com/products/motion-tracking/6-axis/mpu-6050/.